

# Molecular mechanics of the formation of cholic acid micelles

Wou Seok Jou and Paul W. Chun

Department of Biochemistry and Molecular Biology, College of Medicine, University of Florida, Gainesville, FL, USA

*The molecular mechanics of cholic acid micelle formation were simulated using the Sybyl energy minimization program (MAXIMIN2), developed by Tripos Associates, interfaced with micro-Vax.*

*Before energy minimization, the molecular dimensions of the cholic acid dodecamer  $C_{24}H_{40}O_6$ , in terms of the unit cell axes a, b, and c in the cubic crystal class, had values of 13, 18, and 6.7 Å, respectively. After energy minimization, at 9370 kcal/dodecamer, these values had increased to 21.6, 42.8 and 20.9 Å. At an energy minimization level of 21 626 kcal/dodecamer, the micelle structure is stabilized by hydrophobic interaction, forming distinct horizontal channels along the b-axis, directing the carboxyl and hydroxyl groups toward the surface. These structural changes remain relatively constant as the process of energy minimization continues, down to the lowest energy level we considered, 9370 kcal/dodecamer. The cholic acid layers are highly dissimilar, forming channels of irregular size and shape in a somewhat helical structure. The carboxyl groups and phenanthrene rings are in a puckered orientation, which permits compact packing of the sandwiched multilayers.*

*From the dimension of the channels, it is apparent that guest molecules, such as phospholipid, cholesterol, or inorganic calcium, can be incorporated into the micelle through more than one channel, forming inclusion complexes, such as gallstones.*

**Keywords:** bile salts, micellization

## INTRODUCTION

The enterohepatic circulation of bile salts is a dynamic biochemical process involving hepatocytes, canaliculus and bile ductules as concentrated bile is delivered to the intestinal lumen for fat emulsification. Bile salts are derived from cholesterol and their formation is the principal route of cholesterol degradation and elimination in lumen.<sup>1</sup>

The micellization properties of bile salts—sodium deoxycholate (DOC), sodium cholate (CHO), lithocholic acid (LCO), and chenodeoxycholic acid (CDOC)—differ sig-

nificantly from ordinary aliphatic surfactants, such as lauryl sodium sulfate (SDS), sodium decylsulfate ( $Na^+C_{10}DS$ ), tetradecyltrimethyl ammonium bromide (TTAB), or non-ionic surfactants, in that they are restrained sterically to a rigid structure with a definite hydrophobic side and a hydrophilic side.<sup>2,3</sup>

The salts lie “back-to-back” against each other with the hydrophobic side pointing inwards and the hydrophilic one outwards, forming a sheet structure.<sup>3,4</sup> The aggregation number of such complexes or primary micelles may increase up to approximately 10 at an ionic strength of 0.1, forming relatively small micelles with no liquid-crystal phase.

At concentrations below the critical micelle concentration (CMC), deoxycholate exhibits many characteristic regions, with the change in aggregate shape and aggregation number apparently being a continuous process.<sup>2,5,6</sup> When a large aggregation number (12–18 monomeric units) is reached, it is generally assumed that superaggregation may occur through the formation of multilayers or a shift in molecular orientation, resulting in increased viscoelastic effects in solution at room temperature.<sup>3,5</sup>

Neutral bile acids (cholic acid, deoxycholic acid, lithocholic acid; hydroxylated derivatives of steroid 5 $\beta$ -cholan-24-oic-acid) form channel complexes with a large range of organic compounds.<sup>7–18</sup> These orthorhombic  $P$ -lattices ( $P2_12_12_1$ ) all have a common structural pattern, with channels between successive bilayers into which guest molecules fit.<sup>7,18</sup> The crystal symmetry groups of relative positions of successive deoxycholic acid bilayers shift along the  $b$ -axis. These bilayer shifts cause variations in the size, shape, and orientation of the channels to accommodate particular guest molecules with optimal van der Waal's guest–host interaction.<sup>18</sup>

We have examined the nature and extent of cholic acid bilayer formation and the size, shape, and orientation of channels by simulating the molecular mechanics through energy minimization.

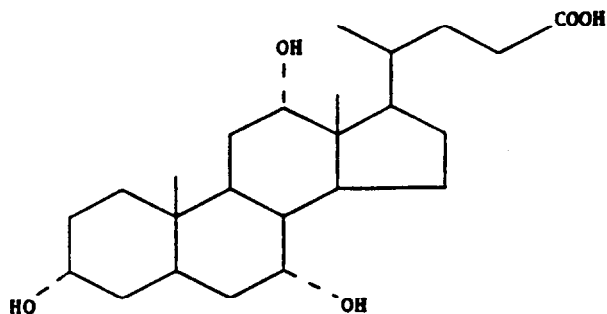
## ENERGY MINIMIZATION PROCEDURE

The molecular mechanics of cholic acid micelle formation were simulated using the SYBYL program developed by Tripos Associates (St. Louis) with an Evans and Sutherland PS390 graphics module interfaced with micro-Vax.

A graphic stick model of the cholic acid monomer, shown in Schematic 1, was stacked vertically without axial rotation to yield 12 layers (dodecamer), as shown in Color Plate 1, by stacking two cholic acid dimers at a distance of 0.71 Å

Address reprint requests to P.W. Chun, Department of Biochemistry and Molecular Biology, College of Medicine, Box J-245, J.H.M.H.C., University of Florida, Gainesville, FL 32610, USA.

Received 4 September 1990; accepted 9 April 1991



Schematic 1. Cholic acid,  $C_{24}H_{40}O_6$ , is incorporated in the SYBYL software and selected as the basic building block for the micelle. It was stacked vertically without axial rotation to yield 12 layers

to form a tetramer. This tetramer formation was stacked three times to yield the final dodecamer form.

Energy minimization procedures were applied to the stacked molecule 50 times (with 100 energy iterations each time), scanning the torsion angles of side chains to relieve steric interactions and to seek a position in which there was no van der Waal's contact between either side of the bond. The energy  $E$  of the molecule in the force field arises through deviations from "ideal" structural features, and can be approximated by a sum of energy contributions:

$$E = \sum E_{\text{str}} + \sum E_{\text{bend}} + \sum E_{\text{oop}} + \sum E_{\text{tors}} \\ + \sum E_{\text{vdw}} + \sum E_{\text{ele}} \\ + \sum E_{\text{dist-c}} + \sum E_{\text{ang-c}} \\ + \sum E_{\text{tor-c}} + \sum E_{\text{range-c}}$$

where the sums extend over all bonds, bond angles, torsion angles, and nonbonded interaction between atoms not bound to each other or to a common atom (i.e., 1,4-interactions and higher).

The bond-stretching, angle-bending torsional, 6–12 Lennard-Jones potential parameters and out-of-plane bending terms for the Tripos 5.3 force field were described by Clark *et al.*<sup>22</sup> The Gasteiger and Marsili method<sup>19–21</sup> was used to calculate the  $\sigma$  and  $\pi$  charges. Here the total  $\sigma$  charge of an atom after the  $k$ th iteration is equal to the sum of charge increments  $Q$  from all bonds, including this atom, and the value of the charge from previous iterations.<sup>22</sup>

The standard SYBYL energy minimizer MAXIMIN2 was used under the following conditions: If the force of an atom exceeded 5 millidynes, an atom-by-atom Simplex minimization was performed until all forces fell below this threshold. After this threshold, conjugate-gradient minimization proceeded until the convergence criterion of a root-mean-square gradient over all atoms of less than 0.1 kcal/mole Å was reached.

MAXIMIN2 uses a combination of first-derivative and nonderivative methods. The Simplex method, a nonderivative-based procedure, is used on an atom-by-atom basis until the maximum force on any atom is below some specified value. In highly distorted structures the potential energy surface and its derivatives are often discontinuous. Simplex can handle these areas while a derivative-based procedure cannot.

The primary optimization methods used in MAXIMIN2 adjust the atomic coordinates of all the atoms simultaneously, based on the first derivative of the energy equation with respect to the degrees of freedom. Aggregates of atoms have six degrees of freedom (three positional and three rotational) while atoms not in aggregates have three variables (the coordinates of the atoms). In mathematical terms, a function of  $n$  variables results in  $n = 6 \times$  the number of aggregates plus  $3 \times$  the number of atoms not in aggregates.

## RESULTS AND DISCUSSION

Energy levels for a single molecule of cholic acid after energy minimization were found to be 36.9 kcal/mol, as shown in Table 1. The molecular dimensions of the axis components  $a$ ,  $b$ , and  $c$  were 15, 10 and 9.32 Å, respectively, which is consistent with values reported by Cobble-dick and Einstein.<sup>14</sup>

Before energy minimization, the energy level of the cholic acid was  $140 \times 10^6$  kcal/dodecamer, almost 95 % of which consisted of van der Waals energy. The energy levels for cholic acid micelles and the molecular dimensions of the coordinates for the cubic crystal class in cholic acid micelles after energy minimization are shown in Table 2. Before energy minimization, the coordinates  $a$ ,  $b$ , and  $c$  for the cholic acid dodecamer had values of 13, 18, and 6.7 Å, respectively. After energy minimization, at 9370 kcal/dodecamer, these values had increased to 21.6, 42.8, and 20.9 Å. As may be seen from Table 2, these values were high at the start of the energy minimization, and decreased exponentially to the minimum energy levels, where the change in energy was reduced to about 15 kcal over a period of 11 CPU hours; see Color Plate 2 and Color Plate 3A.

The width of the  $c$ -axis expanded while the length of the micelle ( $a$ -axis) remained unchanged. Further energy minimization resulted in a continuous reduction in the  $b$ -axis of the molecules, to nearly 43 Å in the energy-minimized form of 9370 kcal/dodecamer (Table 2 and Color Plate 1).

Table 1. Energy levels for a single molecule of cholic acid, before and after energy minimization

Energy of molecule	Cholic acid	
	Before	After (kcal/mol)
Bond stretching energy	16.162	4.504
Angle bending energy	40.324	15.420
Torsional energy	18.771	16.080
Out-of-plane bending energy	0.000	0.003
1–4 van der Waals energy	792.236	6.288
Van der Waals energy	0.776	–1.653
1–4 electrostatic energy	–.244	–2.705
Electrostatic energy	–0.714	–0.964
Total energy	865.311	36.972

**Table 2. Energy levels for cholic acid micelles and molecular dimensions of *a, b, c*, coordinates for the cubic crystal class in cholic acid micelles\***

Before energy minimization				
Molecule	Axis component (Å)			Energy level (kcal/mol)
	<i>a</i>	<i>b</i>	<i>c</i>	
Cholic acid	15.0	10.0	9.32	36.972
Cholic acid: dodecamer	13.0	18.2	6.8	kcal/dodecamer 140 × 10 <sup>6</sup>
After energy minimization				
Cholic acid: micelle (dodecamer)				CPU (hr)
<i>a</i>	<i>b</i>	<i>c</i>	kcal/dodecamer	
24.3	55.6	14.5	1.4 × 10 <sup>6</sup>	241
24.4	55.7	15.8	94,543	124
24.1	54.6	20.9	67,544	112
23.9	53.9	23.1	42,610	101
22.9	42.1	22.6	34,272	96
21.1	42.7	21.4	21,626	84
20.8	42.3	20.0	15,212	60
20.1	42.9	20.1	14,313	48
19.5	42.5	20.4	10,025	40
21.4	42.8	20.8	9,704	30
21.7	42.9	21.0	9,370	20
Total = 835 CPU hrs				

\*If the normal Cartesian coordinate system, which is used throughout SYBYL, is expressed in terms of crystallographic coordinate systems, the parameters defining the cubic class of units are:  $a = b = c = 1.0 \text{ Å}$ , with  $\alpha = \beta = \gamma = 90.0^\circ$

Because the change in energy levels at this point was so slight, we terminated the procedure after 835 CPU hours of batch-wise energy minimization in the micro-Vax system at an energy level of 9370 kcal/dodecamer.

Although the initial stacked micelle structure had a high energy level due to unfavorable steric clashes between cholic acid layers, energy minimization rapidly produced a sterically acceptable structure at 67 544 kcal/dodecamer. At an energy minimization level of 21 626 kcal/dodecamer, the micelle structure was stabilized by hydrophobic interaction, forming distinct horizontal channels along the *b*-axis, pointing the carboxyl and hydroxyl groups toward the surface as shown in Color Plates 2 and 3A.

Color Plate 3A shows the formation of the dodecamer by monomeric unit, starting at the center of the molecule, then building the bottom and top tetramers and incorporating the horizontal channels, which were not significantly altered by an additional 50 CPU hours of energy minimization (Color Plate 3A,B, and C).

Comparison of micelle structure at different energy levels, as shown in Color Plates 1 and 2, indicated that the cholic acid layers were highly dissimilar, stacked in horizontal groups with varying numbers of cholic acid mole-

cules, thus forming channels of irregular size and shape in a somewhat helical structure. Variations in the geometric and structural conformation of individual cholic acid molecules yielded spatial arrangements that differ slightly from their neighbors, as shown in Color Plate 4. Both the carboxyl groups and phenanthrene rings are puckered, an orientation that permits compact packing of the sandwiched multilayers.

Our results confirm Cobbledick and Einstein's<sup>14</sup> conclusions from X-ray diffraction studies, with some evidence of a spiral structure at the top of the cholic acid micelle dodecamer, while the lower segments are in a sandwiched sheet structure incorporating distinct channels. In this energy-minimized form, we see some indication of the 2<sub>1</sub> helices predicted by Campanelli et al.<sup>15</sup> for micelle aggregates in aqueous solution, but not of the bilayer formation reported by Jones et al.<sup>18</sup> in a study of the structure of the 2:1 complex between deoxycholic acid and camphor.

It should be noted that had the layers of dodecamer been stacked differently initially, the final energy-minimized form would show some variation from this structure. From the dimensions of the channels, however, it is apparent that guest molecules such as phospholipid, cholesterol or phenanthrene can be incorporated into the micelle through more

than one channel, forming inclusion complexes, such as gallstones.

## ABBREVIATIONS

$E_{\text{str}}$	Energy of a bond stretched or compressed from its natural bond length
$E_{\text{bend}}$	Energy of bending bond angles from their natural values
$E_{\text{oop}}$	Energy of bending planar atoms out of the plane
$E_{\text{tor}}$	Torsional energy due to twisting about bonds
$E_{\text{vdw}}$	Energy due to van der Waals nonbonded interactions
$E_{\text{ele}}$	Energy due to electrostatic interactions
$E_{\text{dist-c}}$	Energy associated with distance constraints
$E_{\text{ang-c}}$	Energy associated with angle constraints
$E_{\text{tor-c}}$	Energy associated with torsion angle constraints
$E_{\text{range-c}}$	Energy associated with range constraints

## ACKNOWLEDGEMENTS

This work was supported by a grant from the Center for Neurobiology of Aging and in part by a faculty development grant, Division of Sponsored Research, at the University of Florida.

The authors also wish to thank Dr. Roy Vaz of Tripos Associates, St. Louis, MO, for the use of the SYBYL program, and Silicon Graphics, Orlando, FL, for the use of the Silicon Graphics 4D/210GTX graphics module.

## REFERENCES

- Dumont, M., Erlinger, S. and Uchman, S. *Gastroenterology* (1980) **78**, 82–89
- Thomas, D.C. and Christian, S.D. *J. Colloid and Interface Sci.* (1980) **78**, 466–478
- D'arrigo, G., Sesta, B. and La Mesa, C. *J. Chem. Phys.* (1980) **73**, 4562–4566
- Carey, W.C. and Small, D.M. *J. Colloid and Interface Sci.* (1969) **31**, 281–296
- Djavanbakht, A., Kaje, K.M. and Zane, R. *J. Colloid and Interface Sci.* (1974) **78**, 466–478
- Small, D.M. *The Bile Acids*. Plenum, New York, 1971, Chptr. 8, 249–256
- Candeloro De Sanctis, S. *Acta Crystallogr., Sect. B* (1983) **39**, 366–372
- Candeloro De Sanctis, S., Giglio, E., Pavel, V. and Quagliata, C. *Acta Crystallogr., Sect. B* (1972) **28**, 3656–3661
- Candeloro De Sanctis, S., Coiro, V.M., Giglio, E., Pagliuca, S., Pavel, N.V. and Buagliata, C. *Acta Crystallogr., Sect. B* (1978) **34**, 1928–1933
- Candeloro De Sanctis, S. and Giglio, E. *Acta Crystallogr., Sect. B* (1979) **25**, 2650–2655
- Candeloro De Sanctis, S., Giglio, E., Petri, F. and Quagliata, C. *Acta Crystallogr., Sect. B* (1979) **35**, 226–228
- Coriro, V.M., D'andrea, A. and Giglio, E. *Acta Crystallogr., Sect. B* (1980) **36**, 848–852
- D'andrea, A., Fedeli, W., Giglio, E., Mazza, F. and Pavel, N.V. *Acta Crystallogr., Sect. B* (1981) **37**, 368–372
- Cobbledick, R.E. and Einstein, F.W.B. *Acta Crystallogr., Sect. B* (1980) **36**, 287–292
- Campanelli, A.R., De Sanctis, S.C., Giglio, E. and Petriconi, S. *Acta Crystallogr., Sect. C* (1984) **40**, 631–635
- Craven, B.M. and De Titta, G.T. *Chem. Commun.* (1972) **9**, 530–531
- Johnson, P.L. and Schaeffer, J.P. *Acta Crystallogr., Sect. B* (1972) **28**, 3083–3088
- Jones, J.G., Schwartzbaum, S. and Lessinger, L. *Acta Crystallogr., Sect. B* (1982) **38**, 1207–1215
- Gasteiger, J. and Marsili, M. *Tetrahedron* (1980) **36**, 3219–3228
- Gasteiger, J., Saller, H. and Lau, P. *Anal. Chim. Acta* (1986) **191**, 111–123
- Gasteiger, J., Rose, P. and Saller, H. *J. Mol. Graphics* (1988) **6**, 87–92
- Clark, M., Cramer II, R.D. and Van Opdenbosch, N. *J. Comp. Chem.* (1989) **10**, 982–1012